Pergamon

Geochimica et Cosmochimica Acta, Vol. 61, No. 5, pp. 951–963, 1997

0016-7037/97 $17.00 + .00

PII S0016-7037(96)00391-2

Dissolution of Fe(III)(hydr)oxides by metal-EDTA complexes

BERND NOWACK* and LAURA SIGG
Swiss Federal Institute for Environmental Science and Technology (EAWAG) and Swiss Federal Institute
of Technology (ETH), CH-8600 Dübendorf, Switzerland

(*Received December* 28, 1995; *accepted in revised form November* 20, 1996)

Abstract—The dissolution of Fe(III)(hydr)oxides (goethite and hydrous ferric oxide) by metal-EDTA complexes occurs by ligand-promoted dissolution. The process is initiated by the adsorption of metal-EDTA complexes to the surface and is followed by the dissociation of the complex at the surface and the release of Fe(III)EDTA into solution. The dissolution rate is decreased to a great extent if EDTA is complexed by metals in comparison to the uncomplexed EDTA. The rate decreases in the order EDTA $\gg$ CaEDTA > PbEDTA > ZnEDTA > CuEDTA > Co(II)EDTA > NiEDTA. Two different rate-limiting steps determine the dissolution process: (1) detachment of Fe(III) from the oxide-structure and (2) dissociation of the metal-EDTA complexes. In the case of goethite, step 1 is slower than step 2 and the dissolution rates by various metals are similar. In the case of hydrous ferric oxide, step 2 is rate-limiting and the effect of the complexed metal is very pronounced. *Copyright © 1997 Elsevier Science Ltd*

1. INTRODUCTION

Ethylenediaminetetraacetic acid (EDTA) is widely used in industrial processes such as paper manufacturing, electroplating, and photography, and as a powerful complexing agent for metals like Ca, Pb, Zn, or Fe(III).

EDTA is practically not degraded in sewage treatment plants and is present in the effluent in high concentrations of up to 18 μM (Kari and Giger, 1996). EDTA has been measured in rivers (Kari and Giger, 1995), groundwaters (Bergers and deGroot, 1994), and lakes (Ulrich, 1991). In rivers, concentrations up to 0.6 μM were found with typical values between 10 nM and 100 nM (Kari and Giger, 1995). The Fe(III)EDTA fraction of the total EDTA in the effluent from waste water treatment plants is between 20 and 90% (Kari and Giger, 1996), depending upon the dominant metal species used in industry (e.g., the photo-industry uses FeEDTA) and on the complexation reactions during precipitation of phosphate by iron salts. Fe(III)EDTA is degraded photochemically in surface waters with a half-life of several h (Kari and Giger, 1995). Species other than Fe(III)EDTA are stable with regard to photochemical degradation and undergo only slow metal-exchange reactions (Xue et al., 1995).

Infiltration of EDTA to groundwaters may increase the concentration of dissolved heavy metals and assist in their mobilization (Hering, 1995). EDTA and some other complexing agents were also used to decontaminate radioactive equipment from nuclear industry. The waste, containing both complexing agents and radioactive metals like ^{60}Co, was kept underground. EDTA concentrations of up to 31.4 mM have been found in the Hanford site, USA (Toste et al., 1995).

Important interactions of metal-EDTA complexes in aquifers include the adsorption of these complexes to the solid phase and the subsequent dissolution of the sorbent. Iron oxides are of special importance because of their large surface area, their abundance in groundwater aquifers, and the high stability of Fe(III)EDTA formed upon dissolution. Ligands such as oxalate or EDTA are able to promote the dissolution of aluminum and iron oxides by formation of soluble Al- or Fe-ligand complexes (Furrer and Stumm, 1986; Borggaard, 1991). Dissolution of different iron oxides by uncomplexed EDTA has been studied to a great extent previously (Borggaard, 1991; Chang and Matjevic, 1982, 1983; Rubio and Matijevic, 1979; Blesa et al., 1984; Borghi et al., 1989).

In natural systems, strong ligands such as EDTA always occur complexed with metals. Dissolution reactions of iron oxides in the presence of metal-EDTA complexes have been shown to occur in the subsurface environments by Davis et al. (1993) and in the lab-scale experiments by Jardine et al. (1993) and Szecsody et al. (1994). All of these studies have shown the formation of FeEDTA. However, the dissolution reactions of iron oxides in the presence of different metal-EDTA complexes have not yet been studied in detail.

In this study, we have investigated the reactions of uncomplexed EDTA and several metal-EDTA complexes with crystalline α-FeOOH (goethite) and amorphous iron(III)oxide (HFO).

It has often been shown that HFO is dissolved at a faster rate than crystalline oxides when normalized with respect to the surface area (Borggaard, 1991; Deng and Stumm, 1994). Moreover, the exchange kinetics of different metal-EDTA complexes in solution were found to depend strongly on the complexed metal (Xue et al., 1995; Margerum et al., 1978). The effect of different MeEDTA complexes and of the crystallinity of the oxide on the dissolution rate constant will be discussed in this paper.

**Present address:* The Johns Hopkins University, Department of Geography and Environmental Engineering, 373 Ames Hall, 3400 N. Charles Street, Baltimore, Maryland 21218, USA.

2. COORDINATION CHEMICAL MODEL OF DISSOLUTION

Surface complex formation with ligands may polarize the critical metal-oxygen bonds in oxides and can, therefore, enhance the detachment of the metal center from the crystal structure. If these chemical reactions are slow in comparison with transport processes (diffusion), the dissolution kinetics is controlled by the detachment of the metal. Adsorption of the ligand can be described by the surface complexation model. The ligand ($EDTA^{4-}$) adsorbs to specific surface sites ($\equiv$FeOH) by ligand exchange as follows:

$$\equiv\text{FeOH} + \text{EDTA}^{4-} + \text{H}^+ \rightarrow \equiv\text{Fe-EDTA}^{3-} + \text{H}_2\text{O} \quad (1)$$

In the subsequent steps, FeEDTA is detached from the surface. The kinetic rate law of the dissolution depends on the concentration of the activated surface complex. Under steady state conditions, active surface sites reach an equilibrium and are regenerated during the dissolution reaction. The reaction rate can be expressed as follows:

$$d[\text{FeEDTA}^-]/dt = k_1[\equiv\text{Fe-EDTA}^{3-}] \quad (2)$$

where [FeEDTA] is the concentration of Fe(III)EDTA in solution. The overall dissolution rate is the sum of the proton-promoted and the ligand-promoted dissolution (Furrer and Stumm, 1986):

$$d[\text{Fe}]/dt = k_H[\equiv\text{FeOH}_2^+] + k_1[\equiv\text{Fe-L}_1] + k_2[\equiv\text{Fe-L}_2] + \cdots \quad (3)$$

k_H is the rate constant of the proton-promoted and k_1 and k_2 are the rate constants for the ligand-promoted dissolution. L_1 and L_2 represent different ligands and [$\equiv$Fe-L_1] and [$\equiv$Fe-L_2] are their corresponding surface complexes and [Fe] is dissolved Fe(III).

3. MODEL FOR DISSOLUTION BY METAL-EDTA COMPLEXES

Our model for the dissolution of oxides by MeEDTA complexes is shown in Fig. 1. In the case of a metal-EDTA complex ($MeEDTA^{2-}$), the adsorption process can be described in the same way as for the free ligand.

$$\equiv\text{FeOH} + \text{MeEDTA}^{2-} + \text{H}^+ \rightarrow \equiv\text{Fe-EDTAMe}^- + \text{H}_2\text{O} \quad (4)$$

The formation of the ternary surface complex occurs where the ligand (in our case, EDTA) bridges between the surface and the metal (Bowers and Huang, 1986). This complex adsorbs to the surface by ligand exchange with one or more uncoordinated carboxylate groups. The subsequent partial dissociation of the complex leads to the formation of an intermediate species by complexation of the metal and the surface group with the two IDA-parts (iminodiacetic acid) of the EDTA molecule as shown in Eqn. 5. Such intermediate species were found to occur in homogeneous exchange reactions of metal-EDTA complexes (Margerum et al., 1978).

$$\equiv\text{Fe-EDTAMe}^- \rightleftarrows \equiv\text{Fe}\cdot\cdot\text{EDTA}\cdot\cdot\text{Me} \quad (5)$$

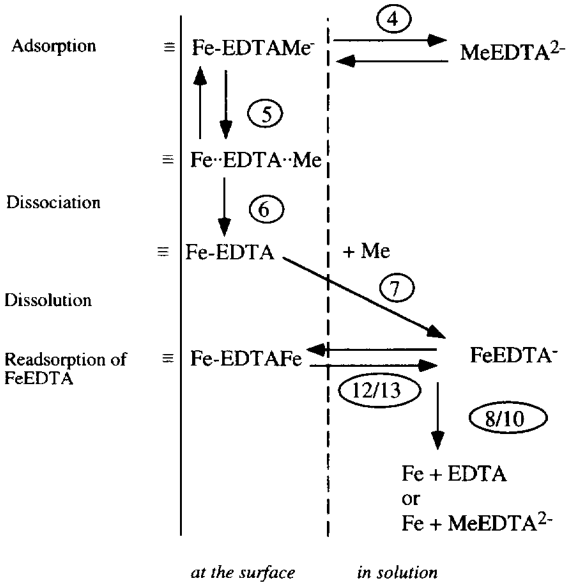

Fig. 1. Schematic representation of the model for the dissolution of oxides by Me-ligand complexes. $\equiv$Fe represents a surface group, $MeEDTA^{2-}$ the metal-EDTA complex and $\equiv$Fe··EDTA··Me the partially dissociated precursor complex which is derived from the adsorbed $\equiv$Fe-EDTAMe. FeEDTA can readsorb to the surface and form a new surface complex different from the precursor complex. The numbers of the reactions correspond to the equations in the text.

Following its formation, the surface complex dissociates and the metal is released (Eqn. 6). The metal may adsorb to the surface or stay in solution, depending upon the pH and the metal.

$$\equiv\text{Fe}\cdot\cdot\text{EDTA}\cdot\cdot\text{Me} \rightleftarrows \equiv\text{Fe-EDTA}^{3-} + \text{Me}^{2+} \quad (6)$$

The released species is assumed to resemble the corresponding dissolved complex (Ludwig et al., 1995). Therefore, we assume that FeEDTA, and not Fe··EDTA··Me, is released, as shown in Eqn. 7.

$$\equiv\text{Fe-EDTA}^{3-} \rightarrow \equiv\text{FeOH(new)} + \text{FeEDTA}^- \quad (7)$$

If the equilibrium solubility concentration of FeEDTA is less than the total EDTA concentration, the back-reactions of FeEDTA have to be considered. For experiments with uncomplexed EDTA, the dissociation of FeEDTA in solution and formation of free EDTA has to be taken into account as follows:

$$\text{FeEDTA}^-(\text{aq}) \rightarrow \text{Fe(III)} + \text{EDTA}^{4-} \quad (8)$$

From Eqns. 7 and 8, the overall dissolution rate becomes

$$d[\text{FeEDTA}^-]/dt = k_1[\equiv\text{Fe-EDTA}^{3-}] - k_{-1}[\text{FeEDTA}^-] \quad (9)$$

where k_1 denotes the dissolution rate constant from and k_{-1} the dissociation rate constant of FeEDTA. For a system with MeEDTA complexes, Eqn. 8 can be written as

$$\text{FeEDTA}^-(\text{aq}) + \text{Me}^{2+}(\text{aq}) \rightarrow \text{MeEDTA}^{2-} + \text{Fe}^{3+} \quad (10)$$

Therefore, the overall dissolution rate becomes

$$d[\mathrm{FeEDTA}]/dt = k_1[\equiv\mathrm{Fe\text{-}EDTA}] - k_{-1}[\mathrm{FeEDTA}]\cdot[\mathrm{Me}] \quad (11)$$

Such reactions were proposed by Lin and Benjamin (1990) for the system of HFO-polyphosphate. They also included adsorption of the dissolution product Fe-polyphosphate into their model. Nowack et al. (1996) have shown that FeEDTA is strongly adsorbed to the HFO surface. We have, therefore, included this reaction into our model. FeEDTA forms two different surface complexes:

$$\equiv\mathrm{FeOH} + \mathrm{FeEDTA}^- + \mathrm{H}^+ \rightarrow \equiv\mathrm{Fe\text{-}EDTA\text{-}Fe} + \mathrm{H_2O} \quad (12)$$

$$\equiv\mathrm{FeOH} + \mathrm{FeEDTA}^- + \mathrm{OH}^- \rightarrow \equiv\mathrm{Fe\text{-}O\text{-}Fe\text{-}EDTA}^{2-} + \mathrm{H_2O} \quad (13)$$

It is, therefore, not sufficient to measure only the dissolved Fe concentration. One has to determine the total concentration of FeEDTA in the system (dissolved and adsorbed FeEDTA as well). Dissolution experiments with HFO and EDTA lead to an underestimation of the total FeEDTA if only the dissolved Fe is determined.

4. MATERIAL AND METHODS

4.1. Reagents and Chemicals

Water was obtained from a Barnstead Nanopure apparatus. All chemicals were analytical grade from Merck or Fluka except HNO_3, NaOH, and $NaNO_3$ which were Merck Suprapur quality. All experiments were done with 0.01 M $NaNO_3$ as the background electrolyte and ambient CO_2-concentrations at room temperature (22–24°C). pH was measured with a Metrohm pH-meter and a Metrohm glass electrode, calibrated with standard buffers.

Metal-EDTA solutions (Zn, Ca, Co(II), Cu, Pb, La, and Ni) were prepared by dissolving the metal-nitrate and $Na_2H_2EDTA \cdot 2H_2O$ in water and boiling for one h. Fe(III)EDTA was prepared by dissolving $NaFeEDTA \cdot 2H_2O$ in water. All stock solutions were 0.01 M.

4.2. Oxides

The goethite was synthesized according to Schwertmann and Cornell (1991). An acidic $Fe(NO_3)_3$-solution was neutralized with NaOH and heated to 60°C for 3 days. The product was washed several times with water and stored as suspension. The goethite was characterized as described in Nowack and Sigg (1996). The BET surface was found to be 21 m^2/g, and $7.95 \cdot 10^{-5}$ M proton-exchangeable surface sites were measured.

HFO was synthesized by rapid hydrolysis of an acidic 0.001 M $Fe(NO_3)_3$-solution with NaOH under conditions where CO_2 was present. The suspension had an ionic strength of 0.01 M $NaNO_3$ and was aged at room temperature and pH 7 ± 0.5 for 16–20 h before use. The surface chemical properties of HFO are described in Nowack et al. (1996). All calculations were done with the average BET surface of 600 m^2/g, the site concentration of 3.75 $\mu M/m^2$ from Dzombak and Morel (1990), and the pK_a-values of 5.08 and 8.09 from Nowack et al. (1996).

4.3. Dissolution Experiments

For experiments with goethite, water, oxide suspension and $NaNO_3$ (0.01 M) were added to 100 mL polyethylene (PE)-bottles. The bottles were acid washed prior to the experiment and wrapped in aluminium foil to avoid any photolysis of Fe(III)EDTA. The pH was adjusted either with HNO_3 (pH below 4), MES (2-morpholinoethane-sulfonic acid)-buffer ($2 \cdot 10^{-3}$ M) for pH 5.2–6.8, HEPES (4-(2-hydroxyethyl)-piperazine-1-ethane-sulfonic acid) ($2 \cdot 10^{-3}$ M) for pH 6.8–8.8, or NaOH for pH > 8.4. The suspensions were equilibrated at the desired pH value for one h before the addition of EDTA. The concentrations were $1.2 \cdot 10^{-5}$ M for EDTA or MeEDTA and 0.11 g/L for goethite. For short time experiments (<6 h), the suspensions were stirred with a Teflon stirrer, and for long time experiments, the suspensions were shaken in a 25°C room in the dark. Aliquots were taken after several time intervals with a PE syringe and filtered through 0.2 μm cellulose nitrate filters (Sartorius), and the filtrates were analysed for EDTA. Subsequently, HNO_3 was added to achieve a final concentration of 0.1 M and the samples were analysed for Fe by graphite tube AAS.

For experiments with HFO, 100 mL PE-bottles wrapped in aluminium foil were used. The same buffers as described above were added and the suspensions were equilibrated for one h at the desired pH value before the addition of EDTA ($1 \cdot 10^{-4}$ M) or MeEDTA ($1.2 \cdot 10^{-5}$ M). The concentration of HFO was $9.4 \cdot 10^{-4}$ M Fe (0.09 g/L) for all experiments. For short-term experiments (<6 h), the suspensions were stirred with a Teflon stirrer, and for long-term experiments, the suspensions were shaken in a 25°C room in the dark. Aliquots were taken in different time intervals with a PE syringe and filtered through 0.2 μm cellulose nitrate filters (Sartorius). The filtrates were analysed for EDTA, and after the addition of HNO_3 to obtain a final concentration of 0.1 M, the metal concentrations were measured by ICP-AES and also by graphite tube AAS for Fe.

In some experiments, 5 mL of the suspension was transferred into a vial with 0.5 mL of 0.1 M phosphate solution to desorb the FeEDTA surface complexes. After 30 min of shaking, this suspension was filtered and analysed for Fe by ICP-AES. The equilibrium concentration of FeEDTA was determined using the same procedure. For goethite, the samples were shaken for 4 mo at 25°C in the dark, and for HFO the samples were shaken for 11 days. The goethite samples were filtered as described above and analysed for EDTA. The HFO samples were treated with phosphate after 5 and 11 days for 30 min to desorb all FeEDTA, and Fe concentrations were analyzed.

4.4. Analysis of EDTA

The concentration of EDTA was measured by the HPLC method described in Nowack and Sigg (1996). The different metal-EDTA complexes were exchanged with $Fe(NO_3)_3$ to form Fe(III)EDTA that can be detected by UV-absorption as follows: 1 mL of the sample was evaporated to dryness in an oven at 70–90°C. The residue was dissolved in 1 mL of formate buffer. $Fe(NO_3)_3$ was added in excess and the solution was heated to 90°C for one h (3 h for NiEDTA experiments) in a water bath. The solution was then cooled to room temperature after which a solution of tetrabutylammoniumbromide (TBA-Br) was added. The sample was then transferred into autosampler vials. The Fe(III)EDTA complex was separated on a Lichrocard 250-4 C_{18} column with formate buffer as eluent (0.001 M TBA-Br, 0.005 M sodium formate, 0.015 M formic acid, and 8% acetonitrile, pH 3.3). Detection was made by a UV-detector at 258 nm.

4.5. Data Evaluation

In the goethite-MeEDTA system, linear dissolution rates are always observed. The dissolution rate constant can therefore easily be determined according to Eqn. 2 under the assumption that the surface concentration of EDTA is constant:

$$k = \frac{\dfrac{[d\mathrm{Fe}]}{dt}}{[\equiv\mathrm{Fe\text{-}EDTA\text{-}Me}]} \quad (14)$$

where $[d\mathrm{Fe}]/dt$ is the slope calculated from the dissolved Fe-concentration vs. time plot.

The dissolution rate constants for the experiments with HFO were determined by use of the program Aquasim (Reichert, 1994). Aquasim is a user-friendly program for performing simulations and data analysis (parameter estimation) of aqueous systems. The user composes the configuration of the system and specifies the transformation processes. Equilibrium and dynamic equations were implemented, and dissolution rates and adsorption constants were fitted to the experimental data. For uncomplexed EDTA, the adsorption was described by the Langmuir equation; for the MeEDTA complexes, partitioning constants K_d were used (linear relationship between dissolved and adsorbed concentration). To determine the rate constants and the equilibrium adsorption constants, the concentrations of all aqueous and adsorbed species should be known. This way, the speciation at each time interval is calculated and the corresponding constants are fitted. Initially, the same concentrations of EDTA and metals were added.

Considering that all EDTA molecules are complexed, the measured species are dissolved $FeEDTA_{aq}$; total dissolved $EDTA_{aq}$, which is the sum of $MeEDTA_{aq}$ and $FeEDTA_{aq}$; total dissolved metal (Me_{aq}), which is the sum of $MeEDTA_{aq}$ and Me^{2+}_{aq}. Me^{2+}_{aq} is the sum of all metal species that are not complexed with EDTA. The solution species may then be written as follows:

$$[MeEDTA_{aq}] = [EDTA_{aq}] - [FeEDTA_{aq}] \qquad (15)$$

$$[Me^{2+}_{aq}] = [Me_{aq}] - [MeEDTA_{aq}] \qquad (16)$$

The speciation of the bulk phase is therefore known. The speciation at the surface cannot be determined from these values. One of the surface species has to be either calculated or determined analytically. We have measured the total concentration of FeEDTA after desorption of the adsorbed FeEDTA. Nowack and Sigg (1996) have shown that phosphate can compete with MeEDTA species adsorbed at the goethite surface. 1 mM phosphate was able to desorb all of the surface complexes such as FeEDTA, PbEDTA, or EDTA, which made possible the determination of FeEDTA. In a previous experiment, we studied the desorption of FeEDTA from HFO with phosphate. At pH 6.6, a 1 mM phosphate concentration was able to desorb within 2 min 96%, and within 30 min 98% of the initially adsorbed $1.17 \cdot 10^{-5}$ M FeEDTA.

The concentrations of the adsorbed MeEDTA and metals were then calculated as follows:

$$[FeEDTA_{ads}] = [FeEDTA_{tot}] - [FeEDTA_{aq}] \qquad (17)$$

$$[MeEDTA_{ads}] = [EDTA_{tot}] - [FeEDTA_{tot}] - [MeEDTA_{aq}] \qquad (18)$$

$$[Me_{ads}] = [Me_{tot}] - [MeEDTA_{aq}] - [MeEDTA_{ads}] - [Me^{2+}_{aq}] \qquad (19)$$

For the experiments with HFO and uncomplexed EDTA, the kinetics of the adsorption were also included in the calculations for the rate constant:

$$d[EDTA_{ads}]/dt = k_{ads}[EDTA_{aq}]([Ads_{max}] - [EDTA_{ads}]) \qquad k_{ads}\ [L \cdot mol^{-1} \cdot s^{-1}] \qquad (20)$$

where $[Ads_{max}]$ is the equilibrium surface concentration of EDTA calculated for each pH value by the Langmuir equation, k_{ads} is the rate constant, and $[EDTA_{ads}]$ and $[EDTA_{aq}]$ are the concentrations of the adsorbed and the dissolved EDTA, respectively. Ads_{max} was calculated by the Langmuir equation as follows:

$$[Ads_{max}] = EDTA_{tot} \frac{K \cdot [EDTA_{aq}]}{1 + K \cdot [EDTA_{aq}]} \qquad (21)$$

where K is the Langmuir adorption constant and $EDTA_{tot}$, the total surface sites for EDTA. For the experiments with MeEDTA, the surface concentration of MeEDTA can be modeled by using a linear relationship of the following form:

$$[Ads_{max}] = [MeEDTA_{aq}]K_d \qquad (22)$$

where K_d is the partitioning constant. The following three equations for the dissolution kinetics, Eqn. 9, adsorption kinetics, Eqn. 20, and Langmuir adsorption isotherms, Eqn. 21 can explain the dissolution behavior of uncomplexed EDTA quite well. The rate constant, k_{ads}, from Eqn. 20 was set to 300 $[L \cdot mol^{-1} \cdot s^{-1}]$ for all pH values.

5. RESULTS

5.1. Equilibrium Concentration of FeEDTA

Determination of the equilibrium concentrations involves the solubility of HFO, hydrolysis of the metal, formation and speciation of FeEDTA, and speciation of MeEDTA. Figure 2a shows the calculated concentrations of FeEDTA as a function of pH for CuEDTA, PbEDTA, and CaEDTA. CuEDTA and PbEDTA are the most stable species at low pH, whereas CaEDTA is only prevalent at pH above 8. FeEDTA and uncomplexed metals, however, adsorb to the surface of iron oxides. These reactions have to be considered. Adsorption of Me^{2+} and FeEDTA was calculated with the constants from Table 1. Figure 2a shows that the FeEDTA-edges for CuEDTA and PbEDTA are shifted towards higher pH, and, especially in the system with PbEDTA, the shape of the curve has changed due to the strong adsorption of Pb^{2+} onto the HFO. Experimental results are shown for CuEDTA and CaEDTA. The MeEDTA was equilibrated with HFO for 11 days and the total amount of FeEDTA was determined after desorption with phosphate. Figure 2a shows the results for HFO. The calculated FeEDTA-edge (K_{SO} of HFO: −38.8) can very well explain the observed Fe concentration for CaEDTA. There is little change between 5 and 11 days, indicating that the dissolution reactions were almost complete after 5 days. The system with CuEDTA shows a different behavior. There is more Fe in the solution than predicted from equilibrium calculation, possibly due to the presence of some Cu^{2-} bound to the strong surface sites (our modeling of adsorption of Cu^{2+} to HFO only involved weak sites). It would also be possible that at pH values around 7, small Fe-particles pass the 0.2 μm filter and are dissolved in the acid. Inorganic dissolved Fe in a system without EDTA was only detected at pH below 4.

The data for CaEDTA or CuEDTA and goethite are shown in Fig. 2b. CaEDTA did not reach the theoretical equilibrium at pH of 6 after 4 mo. CuEDTA is far more stable at low pH than when in contact with HFO. FeEDTA was detected only at pH 4.6, in agreement with the calculated equilibrium.

5.2. Dissolution of Goethite by Uncomplexed EDTA

The dissolution rate of goethite by uncomplexed EDTA becomes faster with increasing pH with a maximum at around pH 8 (Nowack and Sigg, 1996). This behavior can be explained by the formation of two different surface complexes of EDTA: a binuclear complex at low pH and a mononuclear complex at higher pH (Nowack and Sigg, 1996). It was proposed by Stumm and coworkers that a binuclear surface complex inhibits the dissolution, while a mononuclear one enhances it (Bondietti et al., 1993; Biber

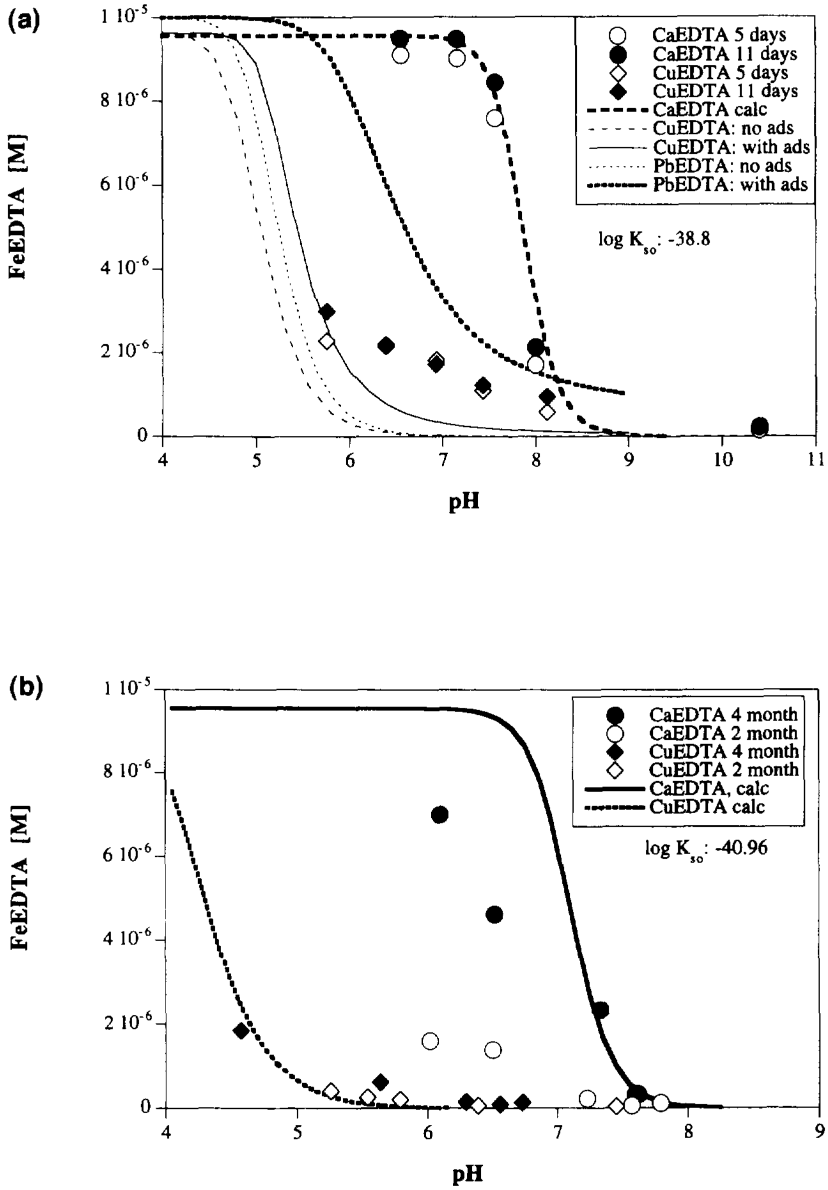

Fig. 2. Extent of dissolution of HFO by CuEDTA and CaEDTA after 5 and 11 days, respectively. Total FeEDTA was measured after desorption with 1 mM phosphate. The lines are calculated with the constants from Table 1 and from Martell and Smith (1974) by MICROQL (Müller, 1993). The FeEDTA-edges of CuEDTA, CaEDTA and PbEDTA without considering adsorption and the ones of CuEDTA and PbEDTA with adsorption of the metal and FeEDTA are shown. The FeEDTA-edges are calculated with a log K_{SO} of −38.8. CuEDTA, CaEDTA $9.6 \cdot 10^{-6}$ M, HFO $9.6 \cdot 10^{-4}$ M Fe, additional Ca (in the CaEDTA experiment) $9.6 \cdot 10^{-5}$ M, 0.01 M $NaNO_3$. (b) Extent of dissolution of goethite by CaEDTA and CuEDTA after 2 and 4 months, respectively. The FeEDTA-edges are calculated with a log K_{SO} of −40.96 (Martell and Smith, 1974). CuEDTA or CaEDTA $9.6 \cdot 10^{-6}$ M, goethite 0.12 g/L, additional Ca (in the CaEDTA experiment) $9.6 \cdot 10^{-5}$ M.

et al., 1994). The dissolution of goethite by EDTA can be modeled by the following expression:

$$\text{rate} = 4.5 \cdot 10^{-7}[\equiv \mathrm{Fe_2\text{-}EDTAH}] + 1.9 \cdot 10^{-5}[\equiv \mathrm{Fe\text{-}EDTA}] \quad [\mathrm{mol\ Fe \cdot s^{-1}}] \qquad (23)$$

The rate constant for the binuclear complex was determined over the pH range 3–6, and the rate constant for the mononuclear complex was determined at around pH 8. The dissolution rate by the mononuclear complex is about 40 times faster than by the binuclear complex. The calculated dissolution rate from Eqn. 23 can explain this behavior rather well, as can be seen from Fig. 3. The concentrations of the surface species $\equiv Fe_2$-LH and $\equiv$Fe-L were calculated with the log K values from Nowack and Sigg (1996), which are shown in Fig. 3. Differences between measured and calculated dis-

Table 1. Log *K* values for adsorption of metals ($\equiv FeOH + Me \rightleftarrows \equiv FeOMe + H^+$) and FeEDTA [Eqns. 12, 13] (Nowack et al., 1996) to HFO, determined by FITEQL (Westall, 1982). Model: constant capacitance.

Surface complex	log *K*
Cu	−0.77
Pb	−0.31
Ca	−5.63
≡Fe-EDTA-Fe	9.17
≡Fe-O-Fe-EDTA	−1.49

solution rate are due to the fact that the total amount of the adsorbed EDTA is a key factor in the model.

5.3. Dissolution of Goethite by AlEDTA

As for the uncomplexed EDTA, the dissolution rate of goethite by AlEDTA increases with increasing pH (Fig. 4). In the system Al-EDTA-goethite, the adsorption edge was explained by the formation of a surface complex of the uncomplexed EDTA (Nowack et al., 1996). AlEDTA was therefore dissociated and only uncomplexed EDTA was adsorbed. Because the surface species in the system are $\equiv Fe_2EDTAH$ and $\equiv FeEDTA$, the dissolution behavior is determined by these complexes and is therefore similar to that of uncomplexed EDTA. However, if the dissolution rate is calculated with the constants from Eqn. 23 for the two surface complexes and with the log *K* values for the surface complexes from Nowack and Sigg (1996), the calculated dissolution rate is about 2–3 times smaller than observed. It must be noted that the adsorption constants for EDTA were obtained from experiments with very low surface coverage of EDTA. The dissolution experiments were done under much higher EDTA concentrations and less goethite than the adsorption experiments (Nowack and Sigg, 1996). It may, therefore, be possible that other surface complexes or another distribution of the surface complexes occurred. Nevertheless, the model does explain the increase in the dissolution rate quite reasonably, as well as the order of magnitude of the dissolution rate. The dissolution rate is slower than in the system with uncomplexed EDTA because only part of the AlEDTA is dissociated. The surface concentration of EDTA is smaller and, therefore, the dissolution rate as well. The non-zero intercept, especially at pH 8, may be due to the heterogeneity of the goethite surface (Furrer and Stumm, 1986). A small amount of amorphous Fe on the surface of the goethite can be dissolved at a faster rate.

5.4. Dissolution of Goethite by Other Metal-EDTA Species

The dissolution of goethite by ZnEDTA shows a behavior that is expected from experiments with simple organic ligands as described in Furrer and Stumm (1986). The dissolution rate decreases with increasing pH, which can be related to the decrease in adsorbed ZnEDTA. ZnEDTA is expected to form only one mononuclear surface complex (Nowack and Sigg, 1996). Above pH 6.5, the dissolution becomes very slow and at pH 7, hardly any dissolution can be detected. At this pH, the equilibrium speciation in the system goethite-Zn-EDTA is favored on the side of ZnEDTA. The mean dissolution rate for ZnEDTA is about

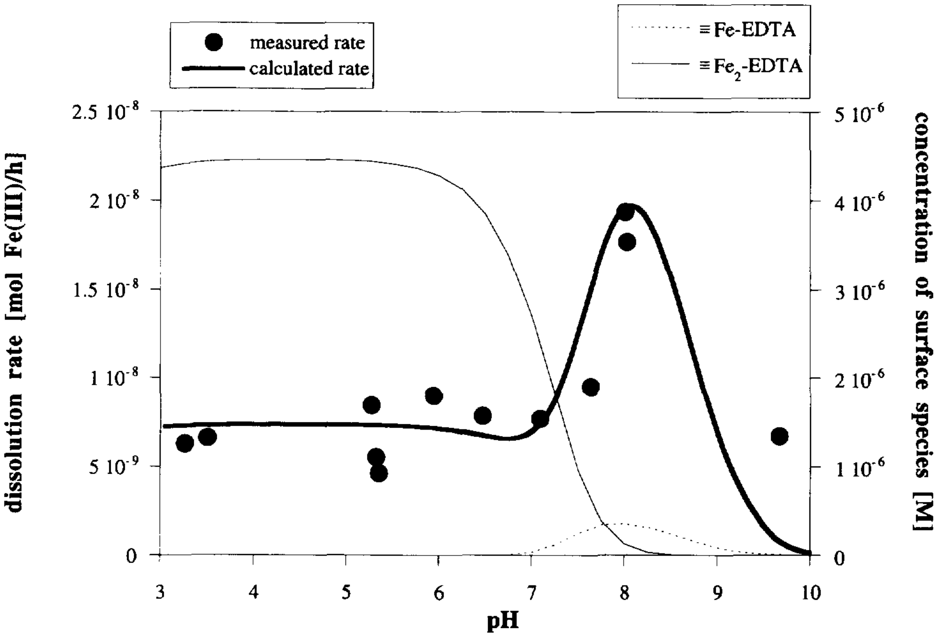

Fig. 3. Dissolution rate [mol Fe(III) · h^{-1}] of goethite by uncomplexed EDTA as a function of pH, comparison of observed and calculated values (Eqn. 23). The concentration of adsorbed EDTA is calculated with the log *K* values from Nowack and Sigg (1996) (thin lines). Goethite 0.12 g/L, EDTA $1.15 \cdot 10^{-5}$ M, 0.01 M $NaNO_3$.

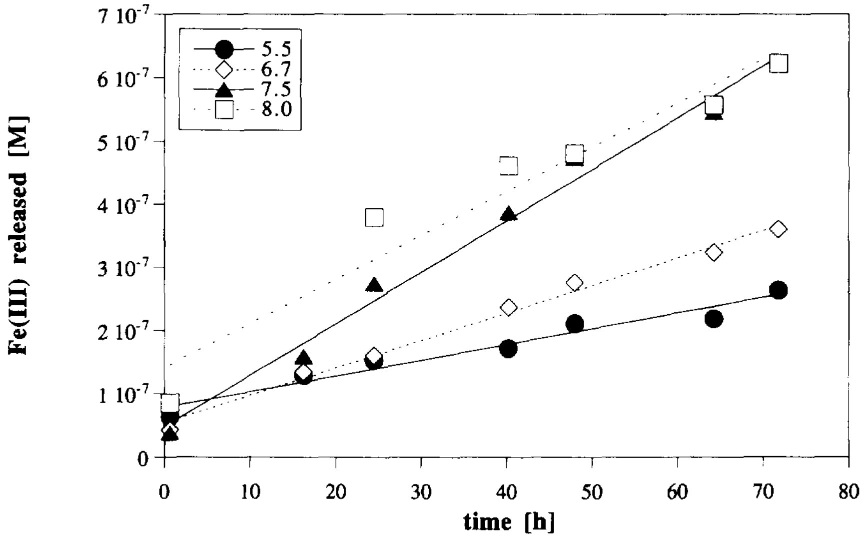

Fig. 4. Dissolution of goethite by AlEDTA at different pH-values. Goethite 0.12 g/L, AlEDTA $1.15 \cdot 10^{-5}$ M, 0.01 M $NaNO_3$.

the same as for the binuclear surface complex of the uncomplexed EDTA (Table 2).

In Fig. 5, the dissolution behavior of several MeEDTA complexes at pH 5.3 is shown. The faster dissolution rate of free EDTA can be related to the higher amount of adsorbed EDTA compared to ZnEDTA. CuEDTA and PbEDTA show similar small rates, whereas the dissolution rate in the presence of NiEDTA is even smaller. Dissolution by CaEDTA was investigated in the pH range from 6.5 to 8. In contrast to ZnEDTA, CaEDTA can dissolve goethite at pH values around 7. At pH 7.3 however, no dissolution was observed. At this pH, the adsorbed EDTA concentration is very low. The dissolution rate for CaEDTA is the same as for ZnEDTA and for the binuclear complex of free EDTA.

5.5. Dissolution of HFO by Uncomplexed EDTA

The dissolution rate of HFO by the uncomplexed EDTA is very fast. In order to follow the formation of FeEDTA, the concentration of EDTA was increased tenfold to $1 \cdot 10^{-4}$ M. Around pH 6, the reaction was complete within 20 min. The amount of adsorbed FeEDTA cannot be determined by the addition of phosphate to the suspension because even in the presence of 0.1 M phosphate, there is still significant dissolution by EDTA. The dissolution rate is, therefore, slightly higher than shown. The dissolved FeEDTA concentration after 20 min is, however, about 90% of the total added EDTA. Figure 6 shows the measured and calculated dissolution behavior at different pH-values. At pH of 9.4, where fast dissolution takes place, the dissolution can be described by zero order kinetics similar to the goethite experiments. Under the conditions of this experiment, the surface concentration of EDTA is very small and an excess concentration of the dissolved EDTA maintains a constant surface concentration. The rate constant cannot be determined at this pH due to the very low concentration of the adsorbed EDTA. Measured and calculated concentrations for dissolved EDTA, adsorbed EDTA, and dissolved FeEDTA at pH 6.25 are shown in Fig. 7. The rate constants are given in Table 3.

Table 2. Rate constants of the dissolution of goethite by MeEDTA-complexes [s^{-1}].

Species	pH	Rate constant [s^{-1}]
$\equiv Fe_2$ EDTA	3–6	$4.5 \cdot 10^{-7}$
$\equiv$Fe-EDTA	8	$1.9 \cdot 10^{-5}$
ZnEDTA	5.3	$3.5 \pm 0.6 \cdot 10^{-7}$
CaEDTA	6.7	$4.4 \cdot 10^{-7}$
CuEDTA	5.3	$1.4 \pm 0.5 \cdot 10^{-7}$
PbEDTA	5.3	$1.8 \pm 0.5 \cdot 10^{-7}$
NiEDTA	5.3	$9.6 \pm 6.1 \cdot 10^{-8}$

5.6. Dissolution of HFO by ZnEDTA

The dissolution rate of HFO by ZnEDTA is much slower than by free EDTA. In Fig. 8, the speciation during dissolution is shown at pH 5.9. Measured concentrations of dissolved and total FeEDTA, dissolved Zn, and total dissolved EDTA facilitated the calculation of the concentrations of the adsorbed species (FeEDTA, ZnEDTA, and Zn^{2+}) and the dissolved species ZnEDTA and Zn^{2+}. It can be seen that the dissolved FeEDTA is only about 30% of the total FeEDTA in the system. Adsorption of FeEDTA can be described at this pH by a K_d value of 1.72. The adsorbed Zn^{2+} concentration is very low at this pH. The dissolved Zn^{2+} is a good tracer for the dissolution reaction because for each mole of FeEDTA, one mole of Zn^{2+} is formed. The adsorption kinetics of ZnEDTA was included. Exclusion of this process, however, does not change the dissolution rate significantly because the timescale of the experiment is much longer than for EDTA.

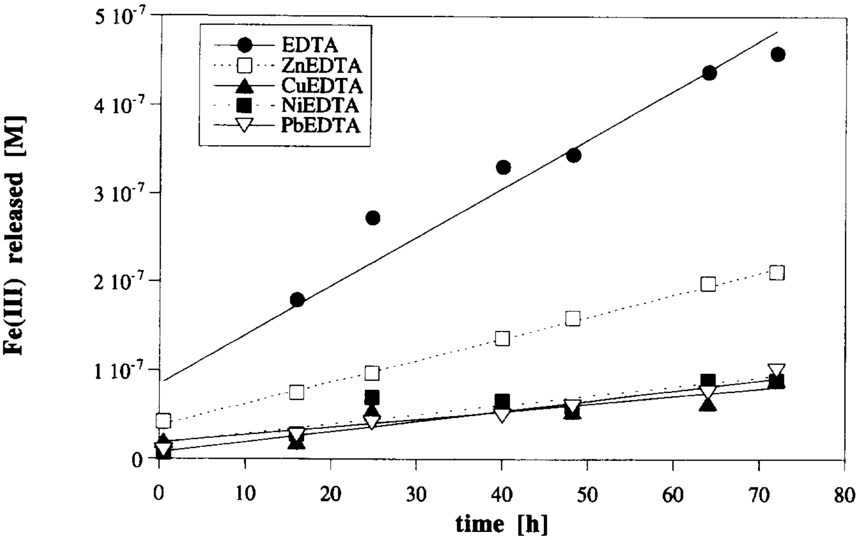

Fig. 5. Dissolution of goethite by MeEDTA-species at pH 5.3. Goethite 0.12 g/L, MeEDTA $1.15 \cdot 10^{-5}$ M, 0.01 M $NaNO_3$.

In Fig. 9, data are shown for the dissolution of HFO by ZnEDTA at different pH values. An important parameter in modeling is the back reaction of FeEDTA with Zn^{2+}. The values for k_{-1} are also given in Table 3, where the dissolution rate constants are summarized. Different batches of HFO may give different dissolution rates (at pH 6 up to factor 3, from 0.0026 to 0.0069). This is probably due to the slightly different oxide properties (e.g., different pH during aging).

5.7. Dissolution of HFO by Other Metal-EDTA Complexes

CaEDTA is able to dissolve HFO at pH values well above 7. At pH 7.1, the dissolution is complete after several h. At pH 8, the dissolution is very slow, but still measurable (Fig. 10). Because the amount of the adsorbed CaEDTA is constant during the duration of the experiment, the formation of FeEDTA follows zero order kinetics. The dissolution rate is about 7 times faster than for ZnEDTA (see Table 3). In this experiment, additional Ca was added to provide a final concentration of $1.2 \cdot 10^{-3}$ M. Without this Ca addition, the dissolution is much faster because, even at high pH, a certain amount of EDTA is not complexed by Ca. The dissolution rate is then the sum of the dissolution rates by free EDTA and CaEDTA.

In Fig. 11, dissolution is shown for several metal-EDTA complexes. LaEDTA dissolves faster than ZnEDTA, but ad-

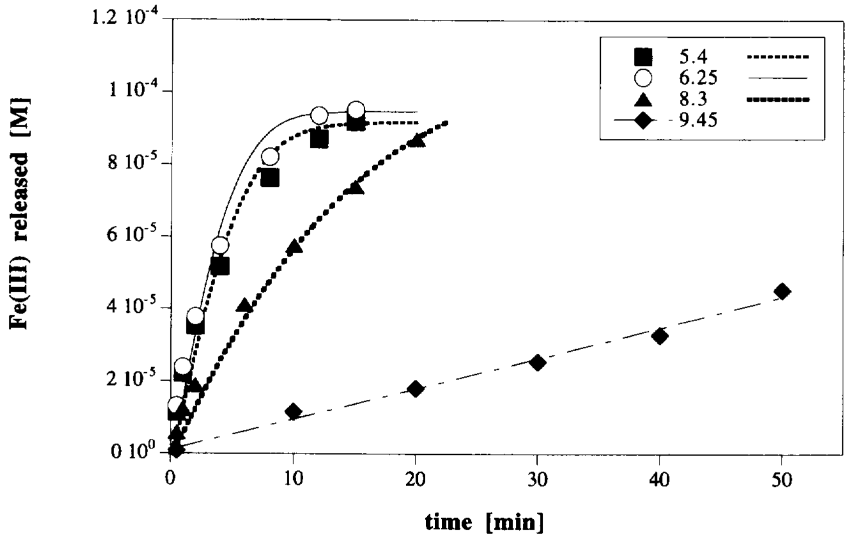

Fig. 6. Dissolution of HFO by uncomplexed EDTA at different pH-values. The lines at pH 5.38, 6.27, and 8.32 are calculated with the rates from Table 3 and with Langmuir adsorption constants for Eqn. 20. The line at pH 9.43 is the linear regression. HFO $9.6 \cdot 10^{-4}$ M Fe, EDTA $1.17 \cdot 10^{-4}$ M, 0.01 M $NaNO_3$.

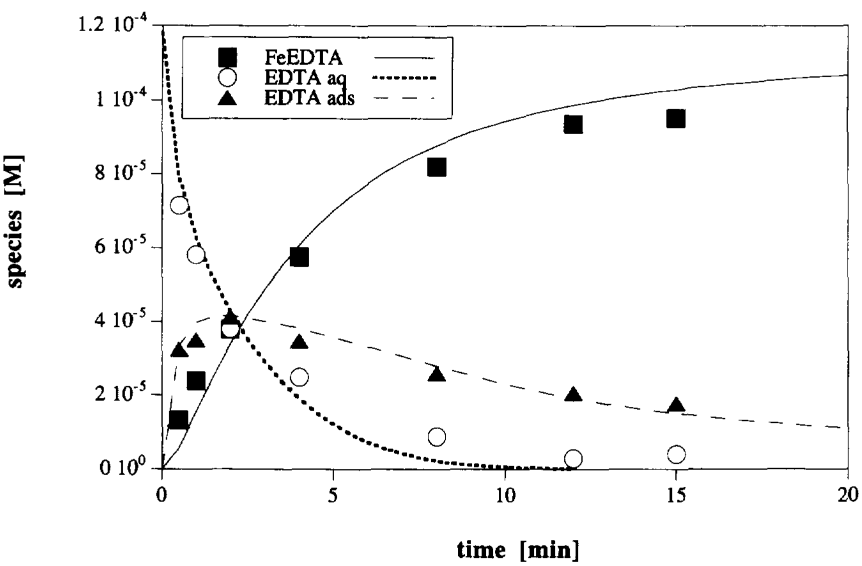

Fig. 7. Dissolution of HFO by uncomplexed EDTA at pH 6.27. Concentrations of dissolved EDTA, dissolved FeEDTA, and adsorbed EDTA ($\equiv$Fe-EDTA) are calculated with the rates from Table 3, with Langmuir adsorption constants (Eqn. 21) and with adsorption kinetics according to Eqn. 21. HFO $9.6 \cdot 10^{-4}$ M Fe, EDTA $1.17 \cdot 10^{-4}$ M, 0.01 M $NaNO_3$.

sorption of this complex is very strong (Nowack and Sigg, 1996). The dissolution rate is the same as for ZnEDTA (Table 3). The faster formation of FeEDTA is due to the higher surface concentration of LaEDTA compared to ZnEDTA. PbEDTA dissolves much faster than the other species and has almost the same dissolution rate as CaEDTA. Co(II)EDTA and CuEDTA have the slowest dissolution rate.

Table 3. Rate constants of the dissolution of HFO by MeEDTA-complexes. k is the dissolution rate constant, k_{-1} the backreaction rate constant according to Eqn. 11 and $FeEDTA_{tot}$ the maximum concentration of FeEDTA.

Species	pH	k_{-1} [$L \cdot mol^{-1} \cdot s^{-1}$]	k [s^{-1}]	$FeEDTA_{tot}$ [M]
EDTA	5.4	0.10[1]	0.35	$1.18 \cdot 10^{-4}$
	6.25	0.13[1]	0.53	$1.18 \cdot 10^{-4}$
	8.3	0.05[1]	0.70	$1.18 \cdot 10^{-4}$
			0.53 ± 0.18	
ZnEDTA	5.25	7	0.0052	$1.2 \cdot 10^{-5}$
	5.85	780	0.0053	$6.1 \cdot 10^{-6}$
	6.25	3255	0.0031	$2.7 \cdot 10^{-6}$
	6.7	6000	0.0035	$2.6 \cdot 10^{-6}$
	6.0	142	0.0046	$6 \cdot 10^{-6}$
	6.0	1001	0.0050	$4.3 \cdot 10^{-6}$
	6.0	624	0.0042	$6.6 \cdot 10^{-6}$
	6.0	500	0.0023	$8.4 \cdot 10^{-6}$
			0.0042 ± 0.0011	
CaEDTA	7.15	0.5	0.034	$1.2 \cdot 10^{-5}$
	7.5	9.25	0.027	$5.5 \cdot 10^{-6}$
			0.031	
CuEDTA	4.8	200	0.0011	$6 \cdot 10^{-6}$
	5.2	300	0.001	$3.9 \cdot 10^{-6}$
	5.95	1500	0.001	$2.5 \cdot 10^{-6}$
	6.45	2000	0.001	$2.4 \cdot 10^{-6}$
			0.001	
PbEDTA	6.0	998	0.025	$8.2 \cdot 10^{-6}$
LaEDTA	6.0	700	0.0049	$6 \cdot 10^{-6}$
Co(II)EDTA	6.0	500	0.00065	$3.2 \cdot 10^{-6}$
NiEDTA	3.7		$7.2 \cdot 10^{-8}$	

[1] in [s^{-1}].

Dissolution by NiEDTA was considerably slower. Measurable amounts of FeEDTA were found only after a few days although at pH 3.7, almost all NiEDTA was adsorbed on HFO. The dissolution rate is about 10^6 times slower than for ZnEDTA and is almost the same as for goethite ($7.2 \cdot 10^{-8}$ s^{-1} for HFO and $9.6 \cdot 10^{-8}$ s^{-1} for goethite, see Tables 2, 3).

6. DISCUSSION

Goethite and HFO are both dissolved by MeEDTA complexes. The two oxides, however, show different dissolution behaviors. The HFO system is dominated by the strong readsorption of FeEDTA to the free surface sites. We have defined "dissolved HFO" as the total concentration of the Fe-ligand in the system, which is the sum of the adsorbed and the aqueous FeEDTA. At the pH values of our study, about 60% of the FeEDTA was readsorbed to the surface. With respect to the total FeEDTA concentration, we always observed linear dissolution rates. Linear dissolution kinetics means that the dissolution is proportional to the amount of the adsorbed ligand. All dissolution rates of HFO in our system are total rates and not apparent rates (occurrence of the FeEDTA in solution). Lin and Benjamin (1990) have shown that the readsorption of the dissolution product can lead to nonlinear dissolution kinetics. The approach of their study is, however, different from that of ours. They defined as "dissolved HFO" only the concentration of the Fe-ligand in the aqueous phase. The nonlinear dissolution kinetics of Lin and Benjamin (1990) is a result of their convention.

For the goethite system, the determination of the dissolved

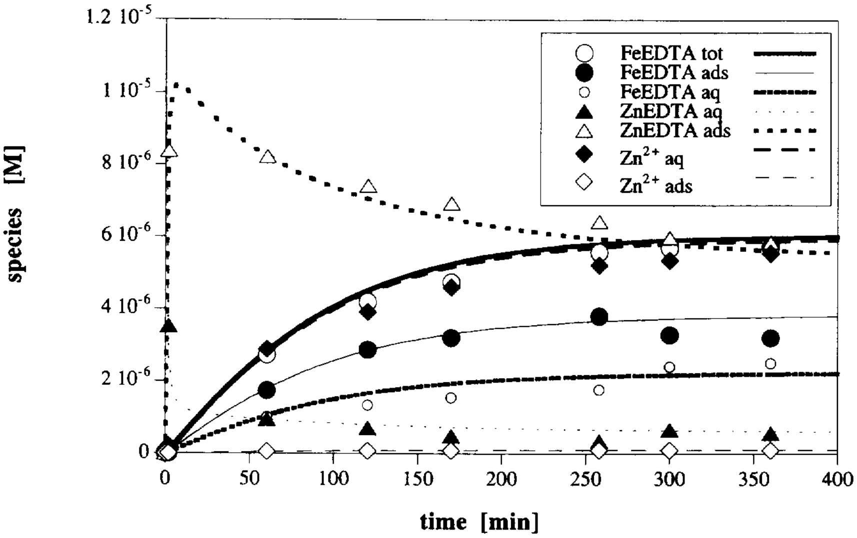

Fig. 8. Dissolution of HFO by ZnEDTA at pH 5.87. Dissolved and total FeEDTA were measured directly and after desorption with phosphate, respectively. Dissolved and adsorbed ZnEDTA and Zn^{2+} are calculated by using Eqns. 19–22 with the measured dissolved Zn and EDTA. The curves are calculated with the rates from Table 3, a K_d-value for the adsorption of Zn^{2+} and a K_d for the adsorption of FeEDTA. HFO $9.6 \cdot 10^{-4}$ M, ZnEDTA $1.2 \cdot 10^{-5}$ M, 0.01 M $NaNO_3$.

Fe is suitable for measuring the dissolution reaction because adsorption of FeEDTA to goethite is almost negligible (Nowack et al., 1996).

The well crystalline goethite is dissolved much more slowly than HFO. Relative dissolution rate constants for different MeEDTA complexes are given in Table 4. The rate constants of MeEDTA complexes are compared to the rate constant of CaEDTA. The ratio of the dissolution rates of HFO and goethite is also shown in Table 4. Dissolution of HFO by the uncomplexed EDTA is $1 \cdot 10^6$ time faster than dissolution of goethite. HFO is also dissolved considerably faster by MeEDTA complexes with the exception of NiEDTA, which has the same rate constant for both oxides. This behavior may be explained by different rate limiting steps in the reaction:

(1) the detachment of the Fe(III) from the crystal structure (Eqn. 7)

(2) the dissociation of the MeEDTA complex at the surface (Eqn. 6).

If step 2 is rate-limiting, then both HFO and goethite

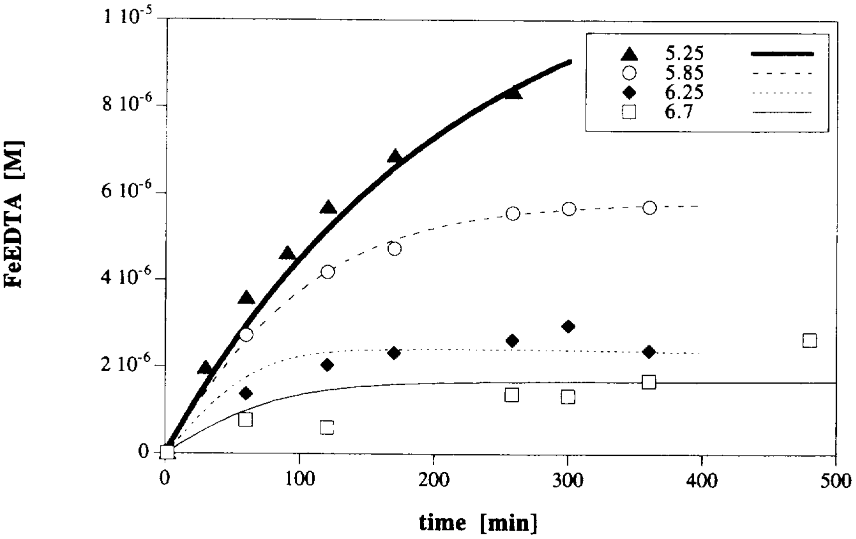

Fig. 9. Dissolution of HFO by ZnEDTA at different pH values. Total FeEDTA was measured after desorption with phosphate. The lines are calculated with the rates from Table 3. HFO $9.6 \cdot 10^{-4}$ M Fe, ZnEDTA $1.2 \cdot 10^{-4}$ M, 0.01 M $NaNO_3$.

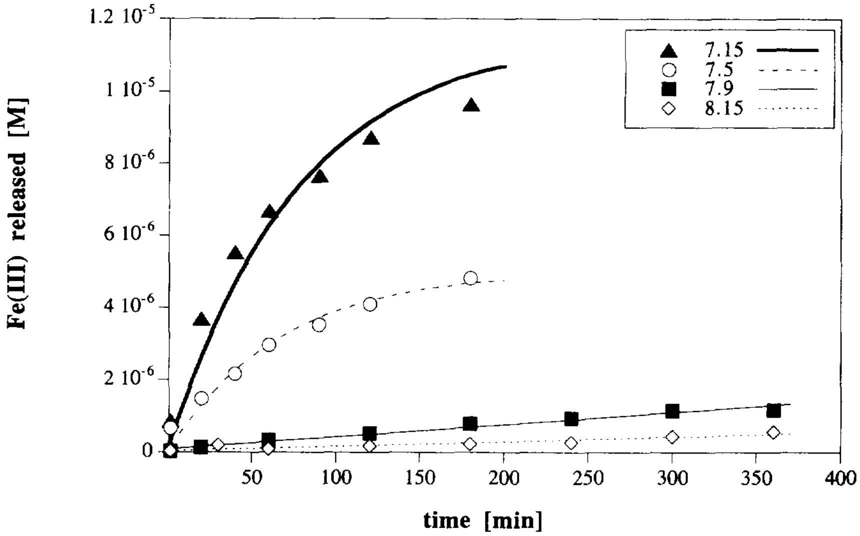

Fig. 10. Dissolution of HFO by CaEDTA at different pH-values. Total FeEDTA was measured after desorption with phosphate. The lines at pH 7.14 and 7.48 are calculated with the rates from Table 3; the lines at pH 7.91 and 8.14 are linear regressions. HFO $9.6 \cdot 10^{-4}$ M Fe, CaEDTA $1.2 \cdot 10^{-5}$ M, Ca $1.21 \cdot 10^{-3}$ M, 0.01 M $NaNO_3$.

should exhibit the same dissolution rate for a given complex. This is the case for NiEDTA which shows dissolution rates of $7.2 \cdot 10^{-8}$ s^{-1} and $9.6 \cdot 10^{-8}$ s^{-1} for HFO and goethite, respectively. If only reaction 1 is rate-limiting, then an oxide should be dissolved by all EDTA-complexes with the same dissolution rate. For HFO, the influence of the MeEDTA on the dissolution rate is more pronounced than for goethite. Goethite is dissolved by ZnEDTA and CaEDTA with almost the same rate and CuEDTA and NiEDTA are within a factor of 5 (Table 4). For goethite, the detachment of Fe(III) from the crystal is, therefore, rate limiting. HFO is dissolved by ZnEDTA 6 times more slowly than by CaEDTA, 30 times more slowly than by CuEDTA, and $5 \cdot 10^5$ times more slowly than by NiEDTA. The influence of the metal is much more pronounced in the case of HFO. This supports the importance of reaction 2 for the HFO-system. The rate limiting step for HFO is therefore the partial dissociation of the surface complex. Reactions of metals with MeEDTA in homogenous solutions have been shown to depend strongly on the complexed metal. CaEDTA reacts fifty-one times faster with Cu^{2+} than ZnEDTA and sixty-three times faster than Co(II)EDTA (Hering and Morel, 1989). No data are, however, available for the homogeneous reaction of MeEDTA with Fe(III) between pH 5 and 7. Due to the presence of

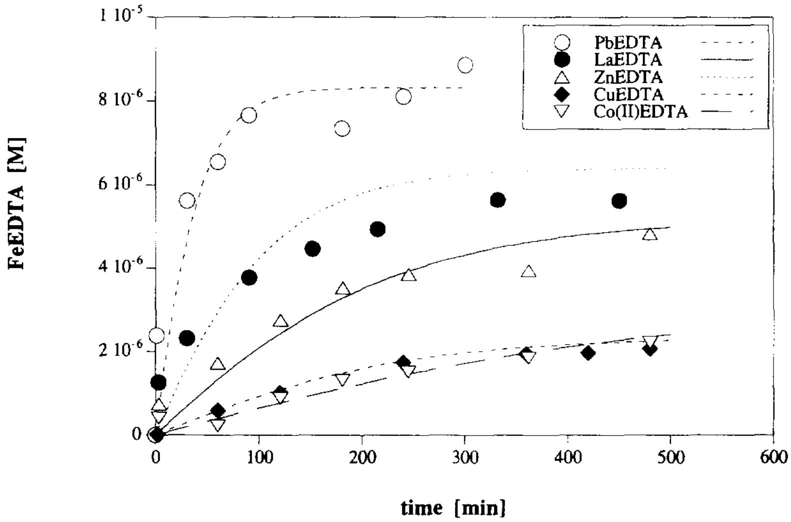

Fig. 11. Dissolution of HFO by metal-EDTA complexes at pH 6.0. Total FeEDTA was measured after desorption with phosphate. The lines are calculated with the rates from Table 3. HFO $9.6 \cdot 10^{-4}$ M, MeEDTA $1.2 \cdot 10^{-5}$ M, 0.01 M $NaNO_3$.

Table 4. Relative dissolution rate constants for different MeEDTA complexes compared to CaEDTA and ratio of the dissolution rate constants for goethite and HFO.

	EDTA	CaEDTA	PbEDTA	ZnEDTA	LaEDTA	CuEDTA	Co(II)EDTA	NiEDTA
Goethite	43.1	1	0.40	0.8		0.32		0.22
HFO	14.1	1	0.81	0.14	0.16	0.03	0.02	$2.3 \cdot 10^{-6}$
HFO/goethite	$1.18 \cdot 10^6$	70300	$1.41 \cdot 10^5$	12450		7150		0.7

different reactions pathways with different metals, reaction rates cannot be compared directly (Margerum et al., 1978).

Metal-exchange in solution occurs mainly by an intermediate where each metal is coordinated to an IDA (iminodiacetate) segment of EDTA. A rough estimate for the dissociation rate for the IDA-segment is the comparison of the water-exchange of the metal and the MeIDA stability constant (Margerum et al., 1978). These ratios show that the slowest segment to dissociate is NiIDA and the fastest is CaIDA. The value of log ($k_{M\text{-}H2O}/K_{MeIDA}$) increases as follows:

$$\underset{-3.72}{\mathrm{Fe(III)}} < \underset{-3.65}{\mathrm{Ni}} < \underset{-1.57}{\mathrm{Cu}} < \underset{-0.64}{\mathrm{Co(II)}} < \underset{0.61}{\mathrm{Zn}} < \underset{2.12}{\mathrm{La}} < \underset{2.43}{\mathrm{Pb}} < \underset{6.19}{\mathrm{Ca}}$$

The corresponding series of dissolution rates is Ni < Co(II) < Cu < Zn < La < Pb < Ca. The good agreement indicates that the dissociation of the $\equiv$Fe· ·L· ·Me complex is rate-limiting.

The results of our study can be applied to aquifer systems. Davis and coworkers (Davis et al., 1993, 1994; Coston et al., 1994) have conducted a large-scale tracer test with PbEDTA, ZnEDTA, CuEDTA, and NiEDTA in a sandy aquifer. They have observed dissolution reactions and the formation of FeEDTA. The observed order of the dissolution rates was PbEDTA > ZnEDTA > CuEDTA $\gg$ NiEDTA. This is the same sequence as in our experiments. Two conclusions can be drawn from their data: (1) MeEDTA complexes behave in the complex aquifer system in the same way as in the well defined batch-system, and (2) the reactive iron oxides in the aquifer are probably amorphous. If they were crystalline, the dissolution rate by the several complexes would be the same. The experiment of Davis and coworkers is therefore not only an excellent example of a possible transfer from the lab to the field scale, but it also indicates that the lab experiments are able to give some new insights into the nature of natural iron oxides.

We can conclude that in a natural system with pH below 6, fast formation of FeEDTA will occur if amorphous Fe oxides are present and if EDTA is not complexed by Ni. A MeEDTA complex that infiltrates to groundwater will therefore be converted to the iron complex after a short residence time. EDTA, therefore, does not enhance the mobility of heavy metals like Pb under acidic conditions.

At pH values of 7 or higher as in calcareous aquifers, the dissolution reactions do not occur or are very slow. At these pH values, MeEDTA complexes are able to migrate over long distances and may enhance the concentration of dissolved metals. Due to its very slow dissolution kinetics, NiEDTA may be transported in groundwater at any pH.

Acknowledgments—This work was supported by the Körber-Stiftung, Hamburg, Germany. Many thanks to Werner Stumm, Christian Ludwig, Aria Amirbahman, and two anonymous reviewers for helpful comments to the manuscript.

Editorial handling: G. Sposito

REFERENCES

Bergers P. J. M. and deGroot A. C. (1994) The analysis of EDTA in water by HPLC. *Wat. Res.* **28,** 639–642.

Biber M. V., Dos Santos Afonso M., and Stumm W. (1994) The coordination chemistry of weathering: IV. Inhibition of the dissolution of oxide minerals. *Geochim. Cosmochim. Acta* **58,** 1999–2010.

Blesa M. A., Borghi E. B., Maroto A. J. G., and Regazzoni A. E. (1984) Adsorption of EDTA and iron-EDTA complexes on magnetite and the mechanism of dissolution of magnetite by EDTA. *J. Colloid Interface Sci.* **98,** 295–305.

Bondietti G., Sinniger J., and Stumm W. (1993) The reactivity of Fe(III)(hydr) oxides: effects of ligands in inhibiting the dissolution. *Colloids and Surfaces* **79,** 157–167.

Borggaard O. K. (1991) Effects of phosphate on iron oxide dissolution in EDTA and oxalate. *Clays Clay Min.* **39,** 324–328.

Borghi E. B., Regazzoni A. E., Maroto A. J. G., and Blesa M. A. (1989) Reductive Dissolution of magnetite by solutions containing EDTA and Fe(II). *J. Colloid Interface Sci.* **130,** 299–310.

Bowers A. R. and Huang C. P. (1986) Adsorption characteristics of metal-EDTA complexes onto hydrous oxides. *J. Colloid Interface Sci.* **110,** 575–590.

Chang H-C. and Matijevic E. (1982) Interactions of metal hydrous oxides with chelating agents. Part V. Magnetite-EDTA. *Finn. Chem-Lett.* **1982,** 90–95.

Chang H-C. and Matijevic E. (1983) Interactions of metal hydrous oxides with chelating agents. IV: Dissolution of hematite. *J. Colloid Interface Sci.* **92,** 479–488.

Coston J. A., Davis J. A., Kent D. B., Hess K., Brienen P., Joye J., and Bussey K. (1994) Multi-species reactive solute transport experiment at the USGS research site, Cape Cod, Massachusetts: 2. reactive transport of metal-EDTA complexes. *EOS* **75,** 249.

Davis J. A., Kent D. B., Rea B. A., Maest A. S., and Garabedian S. P. (1993) Influence of redox environment and aqueous speciation on metal transport in groundwater: preliminary results of tracer injection studies. In *Metals in Groundwater* (ed. M. E. Allen et al.), pp. 223–273. Lewis.

Davis J. A., Kent D. B., Coston J. A., Friedly J. C., Fuller C. C., Anderson L. D., and Hess K. M. (1994) Metal transport in groundwater: From microscopic processes to macroscopic observations. *Proc. American Chemical Society* **34,** 323–326.

Deng Y. and Stumm W. (1994) Reactivity of aquatic iron(III)oxyhydroxydes—implications for redox cycling of iron in natural waters. *Appl. Geochem.* **9,** 23–36.

Dzombak D. A. and Morel F. M. M. (1990) *Surface complexation modeling: Hydrous ferric oxide.* Wiley.

Furrer G. and Stumm W. (1986) The coordination chemistry of weathering: I. Dissolution kinetics of δ-Al_2O_3 and BeO. *Geochim. Cosmochim. Acta* **50,** 1847–1860.

Hering J. (1995) Implications of complexation, sorption and dissolution kinetics for metal transport in soils. In *Metal Speciation and Contamination of Soils* (ed. H. E. Allen et al.). Lewis.

Hering J. G. and Morel F. M. M. (1989) Slow coordination reactions in seawater. *Geochim. Cosmochim. Acta* **53**, 611–618.

Jardine P. M., Jacobs G. K., and O'Dell J. D. (1993) Unsaturated transport processes in undisturbed heterogeneous porous media: II. Co-contaminants. *Soil Sci. Soc. Amer. J.* **57**, 954–962.

Kari F. G., and Giger W. (1995) Modeling the photochemical degradation of EDTA in the River Glatt. *Environ. Sci. Technol.* **29**, 2814–2827.

Kari F. G. and Giger W. (1996) Speciation and fate of ethylenediamninetatraacetate (EDTA) in municipal wastewater treatment. *Wat. Res.* **30**, 122–134.

Lin C.-F. and Benjamin M. M. (1990) Dissolution kinetics of minerals in the presence of sorbing and complexing ligands. *Environ. Sci. Technol.* **24**, 126–134.

Ludwig Ch., Casey W. H., and Rock P. A. (1995) Prediction of ligand-promoted dissolution rates from the reactivities of aqueous complexes. *Nature* **375**, 44–47.

Margerum D. W., Cayley G. R., Weatherburn D. C., and Pagenkopf G. K. (1978) Kinetics and mechanisms of complex formation and ligand exchange. In *Coordination Chemistry* (ed. A. E. Martell); *ACS Monograph 174*, pp. 1–220.

Martell A. and Smith R. (1974) *Critical stability constants*. Plenum.

Müller B. (1993) *MacμQL, V 1.2: A Program to Calculate Chemical Speciation and Adsorption*. EAWAG Kastanienbaum.

Nowack B. and Sigg L. (1996) Adsorption of EDTA and metal-EDTA complexes onto goethite. *J. Colloid Interface Sci.* **177**, 106–121.

Nowack B., Lützenkirchen J., Behra P., and Sigg L. (1996) Modeling the adsorption of metal-EDTA complexes onto oxides. *Environ. Sci. Technol.* **30**, 2397–2405.

Reichert P. (1994) Aquasim—a tool for simulation and data analysis of aquatic systems. *Water. Sci. Technol.* **30**, 21–30.

Rubio J. and Matijevic E. (1979) Interactions of metal hydrous oxides with chelating agents. 1. β-FeOOH-EDTA. *J. Colloid Interface Sci.* **68**, 408–42.

Schwertmann U. and Cornell R. M. (1991) *Iron Oxides in the Laboratory*. VCH.

Szecsody J. E., Zachara J. M., and Bruckhart P. L. (1994) Adsorption-dissolution reactions affecting the distribution and stability of Co(II)EDTA in iron oxide-coated sand. *Environ. Sci. Technol.* **28**, 1706–1716.

Toste A. P., Osborn B. C., Polach K. J., and Lechner-Fish T. J. (1995) Organic analyses of an actual and simulated mixed waste: Hanford's organic complexant site revisited. *J. Radioanal. Nucl. Chem.* **194**, 25–34.

Ulrich M. (1991) Modeling of chemicals in lakes—development and application of user-friendly simulation software (MASAS & CHEMSEE). Diss. ETH, Zurich.

Westall J. C. (1982) FITEQL: A program for the determination of chemical equilibrium constants from experimental data. Tech. Rept., Oregon State Univ., Corvallis.

Xue H. B., Sigg L., and Kari F. G. (1995) Speciation of EDTA in natural waters: Exchange kinetics of FeEDTA in river water. *Environ. Sci. Technol.* **29**, 59–68.